UCSF
UC San Francisco Previously Published Works

Title

Reduced Mural Cell Coverage and Impaired Vessel Integrity After Angiogenic Stimulation in the Alk1-deficient Brain

Permalink

https://escholarship.org/uc/item/1gv0r113

Journal

Arteriosclerosis Thrombosis and Vascular Biology, 33(2)

ISSN

1079-5642

Authors

Chen, Wanqiu
Guo, Yi
Walker, Espen J
et al.

Publication Date

2013-02-01

DOI

10.1161/atvbaha.112.300485

Peer reviewed

Reduced mural cell coverage and impaired vessel integrity after angiogenic stimulation in the *Alk1*-deficient brain

Wanqiu Chen, PhD[1], **Yi Guo, MD**[1], **Espen J. Walker, PhD**[1], **Fanxia Shen, MD**[1], **Kristine Jun, BS**[1], **S. Paul Oh, PhD**[5], **Vincent Degos, MD, PhD**[1], **Michael T. Lawton, MD**[2], **Tarik Tihan, MD, PhD**[4], **Dimitrios Davalos, PhD**[6], **Katerina Akassoglou, PhD**[3,6], **Jeffrey Nelson, MS**[1], **John Pile-Spellman, MD**[7], **Hua Su, MD**[1], and **William L. Young, MD**[1,2,3]

[1]Center for Cerebrovascular Research, Department of Anesthesia and Perioperative Care, University of California, San Francisco, California

[2]Department of Neurological Surgery, University of California, San Francisco, California

[3]Department of Neurology, University of California, San Francisco, California

[4]Department of Pathology, University of California, San Francisco, California

[5]Department of Physiology and Functional Genomics, College of Medicine, University of Florida, Gainesville, Florida

[6]Gladstone Institute of Neurological Disease, University of California, San Francisco

[7]Neurological Surgery P.C., Lake Success, New York

Abstract

Objective—Vessels in brain arteriovenous malformations (bAVM) are prone to rupture. The underlying pathogenesis is not clear. Hereditary hemorrhagic telangiectasia type 2 (HHT2) patients with activin receptor-like kinase 1 (*Alk1*) mutation have a higher incidence of bAVM than the general population. We tested the hypothesis that vascular endothelial growth factor (VEGF) impairs vascular integrity in the *Alk1*-deficient brain through reduction of mural cell-coverage.

Methods and Results—Adult $Alk1^{1f/2f}$ mice (loxP sites flanking exons 4-6) and wild-type (WT) mice were injected with 2×10^7 PFU Ad-Cre and 2×10^9 genome copies of AAV-VEGF to induce focal homozygous *Alk1* deletion (in $Alk1^{1f/2f}$ mice) and angiogenesis. Brain vessels were analyzed eight weeks later. Compared to WT mice, the *Alk1*-deficient brain had more fibrin ($99\pm30\times10^3$ pixels/mm^2 vs. $40\pm13\times10^3$, P=0.001), iron deposition (508 ± 506 pixels/mm^2 vs. 6 ± 49, P=0.04), and Iba1$^+$ microglia/macrophage infiltration (888 ± 420 Iba1$^+$ cells/mm^2 vs. 240 ± 104 Iba1$^+$, P=0.001) after VEGF stimulation. In the angiogenic foci, the *Alk1*-deficient brain had more α-SMA$^-$ vessels ($52\pm9\%$ vs. $12\pm7\%$, P<0.001), fewer vascular associated pericytes (503 ± 179/mm^2 vs. 931 ± 115, P<0.001), and reduced PDGFR-β expression ($26\pm9\%$, P<0.001).

Conclusion—Reduction of mural cell coverage in response to VEGF stimulation is a potential mechanism for the impairment of vessel wall integrity in HHT2-associated bAVM.

Keywords

brain arteriovenous malformation; activin receptor-like kinase 1; pericyte; iron deposition; PDGFR-β

Brain arteriovenous malformations (bAVM) are tangles of abnormal, dilated vessels that directly shunt blood between arteries and veins. Surrounding the AVM nidus, but extrinsic to the lesion, there may be a network of dilated capillaries.[1, 2] The abnormal vessels are prone to rupture and cause life-threatening intracranial hemorrhage. The pathogenesis of bAVM and the exact vascular defects that cause the rupture are not known. Knowledge of the underlying mechanisms could provide critical insights for the development of novel therapies to reduce the risk of life-threatening spontaneous rupture.

AVMs in various organs, including the brain, are common in patients with hereditary hemorrhagic telangiectasia (HHT), an autosomal dominant disorder. The two main subtypes of HHT (HHT1 and HHT2) are caused by loss-of-function mutations in the endoglin (*ENG*) and activin receptor-like kinase 1 (*ALK1*, or *ACVRL1*) genes, both of which participate in TGF-β signaling. These HHT mutations can be viewed as risk factors for bAVM. Compared to the prevalence of sporadic bAVMs in the general population (10/100,000), the prevalence in HHT1 (*ENG*) is 1000-fold higher, and in HHT2 (*ALK1*), 100-fold higher.[3] Previously we created a bAVM model in adult mice through focal *Alk1*-deletion and VEGF stimulation.[4] This model mimics both macroscopic and microscopic morphological features of the human lesional phenotype, including large dysplastic, tangled vessels and arteriovenous shunting. Some abnormal vessels with a diameter larger than 15 μm have no α-SMA positive cells on their wall.[4]

Here, we tested the hypothesis that VEGF stimulation in the *Alk1*-deficient brain impairs vascular integrity through reduction of mural cell-coverage. We demonstrated that compared to wild-type (WT) mice, VEGF stimulation in the *Alk1*-deficient brain not only reduces vascular α-SMA positive cells but also pericytes, which is associated with extravasation of intravascular components. Since the platelet-derived growth factor receptor-β (PDGFR-β)/PDGF-BB signaling pathway has been implicated in regulating pericyte recruitment to newly formed blood vessels, we also analyzed the expression of PDGFR-β and PDGF-BB in the *Alk1*-deficient brain following VEGF stimulation.

Methods

For complete details on Methods and Materials, please refer to the online Data Supplement. The experimental protocols involving animal usage were approved by the Institutional Animal Care and Use Committee (IACUC) of the University of California, San Francisco (UCSF). All studies involving patients were approved by the UCSF Institutional Review Board, and patients gave informed consent.

Animal Model

Adult *Alk1*[1f/2f] mice (exons 4-6 flanked by loxP sites)[5] and C57BL/6 mice were used. The "1f" allele indicates a null allele derived from the conditional (2f) allele by cre-mediated recombination of the 2 loxP sites flanking exons 4-6 in the germ cells. Briefly, the mice were anesthetized with isoflurane and placed in a stereotactic frame with a holder (David Kopf Instruments, Tujunga, CA). A burr hole was drilled in the pericranium 2mm lateral to the sagittal suture and 1mm posterior to the coronal suture. Ad-Cre (2×10^{7} plaque forming

units) and AAV-VEGF (2×10^9 genome copies) were stereotactically injected into the basal ganglia[4] of eight-week-old $Alk1^{1f/2f}$ mice, about 3mm under the surface of the cortex. An additional group received the same amount of the vectors in the cortex (Supplemental Methods and Supplemental Figure S1). Ad-GFP and AAV-LacZ were used as control for Ad-Cre and AAV-VEGF. Cytomegalovirus (CMV) promoter was used to drive Cre and VEGF expression in Ad-Cre and AAV-VEGF vectors. Gene expression was mostly in endothelial cells, neurons and astrocytes.[4, 6] Two control groups with intact $Alk1$ gene were included: (1) wild type (WT) mice injected with Ad-Cre and AAV-VEGF; and (2) $Alk1^{2f/2f}$ mice injected with Ad-GFP and AAV-VEGF. A third control group was $Alk1$-deficient mice that had not been treated with VEGF: $Alk1^{1f/2f}$ mice injected with Ad-Cre and AAV-LacZ.

Statistical Analysis

Data are presented as mean ± standard deviation (SD). For quantification of Prussian blue staining, we used the Kruskall-Wallis test followed by the Wilcoxon rank-sum test. Fisher's exact test was used to analyze the associations of α-SMA negative (α-SMA⁻) vessel/ Prussian blue staining. We measured the linear relationship between vessel-associated pericyte and fibrin deposition, as well as between Iba⁺ cells and Prussian blue-positive area using Pearson's correlation coefficient. The linear relationship between the numbers of $ZIC1^+$ cells and fibrin deposition, as well as Prussian Blue positive area and $Iba1^+$ cells, was determined using a simple linear regression analysis, which generates the corresponding R^2 estimate. Due to the skewed nature of Prussian Blue area and the number of $Iba1^+$ cell count, the data observations were log-transformed prior to performing this analysis. The other data were analyzed using one-way ANOVA to compare the means of each group. A p value < 0.05 was considered statistically significant. Sample sizes were n=6 for each group.

Results

Alk1 Deficiency Potentiates Vascular Integrity Impairment After VEGF Stimulation

Focal $Alk1$-deletion and VEGF stimulation were induced as previously described.[4] Injection of Ad-Cre into the brain of $Alk1^{2f/2f}$ and $Alk1^{1f/2f}$ mice reduced ALK1 expression significantly (Supplemental Figure S5). Two-photon imaging demonstrated the dilated dysmorphic cerebrovasculature in the angiogenic focus of $Alk1^{1f/2f}$ mice that received Ad-Cre and AAV-VEGF in the cortex (Supplemental Figures S1A and B, and S2). The morphology of dysplastic vessels induced in the $Alk1^{1f/2f}$ cortex was similar to that of bAVM in HHT patients (Supplemental Figure S1C and D). To investigate the integrity of the abnormal vessels, we analyzed fibrin deposition in the extra vascular space. When soluble blood protein fibrinogen extravasates in the CNS, it is converted to insoluble fibrin by thrombin.[7] VEGF stimulation resulted in a low level of fibrin deposition on the vessel wall and in the brain parenchyma adjacent to the vessels in the brain of WT mice ($40\pm13\times10^3$ pixels/mm², Figure 1A) and $Alk1^{2f/2f}$ mice ($45\pm16\times10^3$ pixels/mm², P=0.98). Without VEGF stimulation, the $Alk1$-deficient brain had a low level of fibrin deposition ($10\pm5\times10^3$ pixels/mm²). However, significantly more fibrinogen extravasation was detected in the angiogenic foci of the $Alk1$-deficient brain ($99\pm30\times10^3$ pixels/mm², P= 0.001 vs. WT, P= 0.003 vs. $Alk1^{2f/2f}$, Figure 1C). Perivascular fibrin deposition was mostly around the dysplastic vessels (Figure 1B).

In addition to fibrin, we found that the $Alk1$-deficient brain had hemosiderin deposition after VEGF stimulation (Figure 2). Prussian blue staining showed that after VEGF stimulation, $Alk1$-deficient mice had ≈10-fold higher Prussian blue-positive area (508 ± 506 pixels/mm²) compared to WT (61 ± 49 pixels/mm², P=0.04) and $Alk1^{2f/2f}$ mice (51 ± 75 pixels/mm², P=0.03, Figure 2B). Without VEGF stimulation, the $Alk1$-deficient brain had a low level of Prussian blue-positive area (8 ± 13 pixels/mm²). Moreover, red blood cells (RBCs) were

detected in the brain parenchyma outside of the blood vessels in the *Alk1*-deficient brain, with macrophages in the surrounding region clearing RBCs (Figure 2C). Iron deposition was also detected in the nidus and perinidus areas of non-ruptured human brain AVM specimens (Figure 2D), suggesting that vessel leakage could be an important phenotype related to the pathogenesis of the human disease.

Correlation of Iron Deposition with Microglia/Macrophages

To investigate the relationship between inflammation and vascular integrity, we analyzed the number of microglia/macrophages at the angiogenic foci. We found that there were more Iba1$^+$ microglia/macrophages present in the *Alk1*-deficient brain after VEGF stimulation (888±420 Iba1$^+$ cells/mm^2, Figure 3A&B) than in VEGF-treated WT (240±104, P=0.001) and *Alk1*$^{2f/2f}$ mice (429±106, P=0.02), and in untreated *Alk1*$^{1f/2f}$ mice (295±148, P=0.002). Moreover, the number of Iba1$^+$ cells positively correlated with Prussian blue-positive area (R^2=0.2, P=0.029; Figure 3C).

Iron Deposition in Vessels without α-SMA$^+$ Cell Coverage

Smooth muscle cells are α-SMA$^+$ and have an elongated, thin spindle-like shape lining outside the endothelial cells of arteries and veins. In normal conditions, vessels larger than 10 μm usually have one or several layers of smooth muscle cells on their wall. During active angiogenesis, some pericytes are also positive for α-SMA staining.[8] Here, we quantified the percentage of α-SMA$^-$ vessels (>15 μm) in the angiogenic foci, and found that 52±9% vessels were α-SMA$^-$ in *Alk1*-deficient mice, which is significantly more than those in WT (12±7%) and *Alk1*$^{2f/2f}$ mice (15±11%) (Figure 4B, P=0.001). Without VEGF stimulation, the *Alk1*-deficient brain had a similar number (17±9%) of α-SMA$^-$ vessels as VEGF-treated WT and *Alk1*$^{2f/2f}$ (Figure 4B, P>0.05). Interestingly, in the *Alk1*-deficient mice, Prussian blue-positive staining appeared to be mostly located on the wall and the surrounding brain parenchyma of α-SMA$^-$ -dysplastic vessels (Figure 4C). Detailed quantification showed that among vessels larger than 15 μm, 53% of α-SMA$^-$ vessels were located within or near a Prussian blue-positive area; only 9% of α-SMA$^+$ vessels were localized near a Prussian blue-positive area (Figure 4D, P<0.001). This suggests that lack of α-SMA$^+$ cell-coverage is associated with RBC extravasation.

Alk1 Deficiency Leads to Reduced Number of Vessel-associated Pericytes After VEGF Stimulation

To determine whether the impaired vascular integrity in the *Alk1*-deficient brain is also related to the number of pericytes on the vessel wall, we used anti-ZIC1 and anti-NG2 antibodies to identify pericytes. Both NG2 and ZIC1 staining showed that vessels in the *Alk1*-deficient brain have less pericyte coverage after VEGF stimulation (Figure 5A). Since other cell types in the adult brain, i.e. oligodendrocyte progenitor cells, also express NG2,[8] and NG2 positive staining is located on the cytoplasma membrane, it is difficult to quantify vascular-associated NG2 positive cells. ZIC1 has been reported to be a specific marker for pericyte-nuclei in the mouse embryo brain.[9] To test if ZIC1 is pericyte-specific in the adult mouse brain, we performed double immunostaining using the anti-ZIC1 antibody with anti-NeuN, anti-GFAP, and anti-desmin (Supplemental Figure S3). We did not find ZIC1 positive astrocytes; however, some NeuN positive cells in the basal ganglia were ZIC1 positive, suggesting that ZIC1 is expressed by cells other than pericytes in the adult mouse brain. To quantify the vascular-associated pericytes, we only counted the ZIC1$^+$ nuclei located on the vessel wall (Figure 5B).

The number of vascular-associated pericytes in the angiogenic foci of *Alk1*-deficient brain (503±179 ZIC1$^+$ nuclei/mm^2 vessel area, Figure 5C) was approximately 45% less than that in the angiogenic foci of the WT (931±115, P<0.001) and *Alk1*$^{2f/2f}$ (936±145, P<0.001)

mice. *Alk1*-deficient-only did not reduce the number of vascular associated pericytes (888±108, P=0.95). More importantly, the number of pericytes on the vessel wall inversely correlated with the level of fibrin deposition (R^2=0.45, P=0.0003; Figure 5D). This indicates that the reduction of vascular pericytes correlated with impairment of vascular integrity in the lesion.

PDGFR-β Expression is Reduced in the *Alk1*-deficient Brain

To determine if reduced vascular mural cell coverage in the *Alk1*-deficient brain was associated with the reduction of PGDFR-β and PDGF-BB, we analyzed the levels of PDGFR-β and PDGF-BB protein expression. We found that PDGFR-β expression in the angiogenic foci of *Alk1*-deficient brain was reduced as compared to that in the angiogenic foci of WT and *Alk1*[2f/2f] mice (P<0.001; Figure S6B). *Alk1*-deficient brain had a similar level of PDGFR-β with or without VEGF stimulation (P=0.99). There was no difference in PDGF-BB expression among all the groups (P=0.28; Figure S6C).

Discussion

Compared to the mice that have normal *Alk1* gene, we found that the vascular integrity was impaired in the brain of *Alk1*-deficient mice after VEGF stimulation, as evidenced by (a) increased fibrin and iron deposition, (b) small pockets of extravasated RBCs outside of the vessels, and (c) macrophage/microglia infiltration on the vessel wall and in the brain parenchyma near the dysplastic vessels. The dysplastic vessels in the angiogenic foci of *Alk1*-deficient brain displayed less mural cell coverage than the normal cerebrovasculature. Consistent with the reduction of vascular pericytes, PDGFR-β expression in the angiogenic foci of *Alk1*-deficient mice was reduced. Iron deposition was found near the α-SMA⁻ vessels, as well as in the non-ruptured human bAVM specimen. A key finding from our study is that ALK1 plays a role in maintaining the integrity of vessels in the adult brain during angiogenesis; patients with mutations in ALK1 and HHT2-associated bAVM may be prone to the same loss of vascular integrity, as plasma and tissue levels of VEGF appear to be elevated in these patients.[10]

Roughly half of all bAVM patients come to clinical attention with an ICH, and providing protection against the risk of spontaneous ICH after diagnosis is the main reason for invasive therapy.[11] Hemoglobin breakdown products are reabsorbed or cleared by macrophages, and hemosiderin often remains the only sign of a previous hemorrhage.[12] Even with relatively iron-insensitive MR sequences, it is intriguing that ≈ 14%-20% of bAVM patients with non-hemorrhagic history exhibit signs of prior hemorrhage events.[12] We recently described that in patients with unruptured bAVMs and with no prior history of hemorrhage, 30% of resected surgical specimens contain microscopic evidence of hemosiderin in the vascular wall or intervening stromal tissue.[13] The underlying mechanisms for bAVM rupture and microbleeding in unruptured bAVM patients are not fully understood, and might be involved in reduced mural cell coverage. However, the dysplastic vessels in the VEGF-stimulated *Alk1*-difficient brain probably more closely mimics an early developmental stage of HHT2-associated bAVM and perinidal capillaries, rather than the fully formed and mature lesion seen in symptomatic human disease. Further study is needed to analyze pericyte and mural cell coverage in human bAVM. Interestingly, abnormal structural integrity of the perinidal vessels has been suggested. At the microscopic level, there is evidence of abnormal BBB structure, increased vessel permeability, RBC diapedesis, and capillary bleeding in human perinidal bAVM,[1, 14] similar to our findings here.

Inflammatory cell types, e.g., macrophages and neutrophils, have been detected in human bAVM surgical specimens, even in those without a prior history of hemorrhage or previous

treatment with embolization or radiosurgery.[15] Polymorphic genetic variations in several inflammatory cytokines are associated with bAVM hemorrhage.[16] We found that in the angiogenic foci of *Alk1*-deficient mice, the number of macrophage/microglia increased in the lesion, and positively correlated with the degree of iron deposition (Prussian blue-positive area). Moreover, the distribution of macrophages/microglia resembled the pattern of CD68 positive cells in human bAVM: present in and around the dysplastic vessel wall. The number of Iba1^{+} cells positively correlated with the degree of iron deposition. Thus, inflammation might also be involved in HHT2-associated bAVM pathogenesis and rupture of dilated dysplastic vessels. Further experiments are needed to determine the roles of ALK1 in inflammatory pathways.

It has been suggested that ALK1 regulates vascular smooth muscle (vSMC) differentiation and recruitment to the perivascular region during the embryonic stage.[17] In E10.5 *Alk1*^{-/-} mouse embryos, vSMCs were reduced in the dorsal aorta region. In human bAVMs, SMC- vessels (>15 μm) have also been reported.[4] Taken together with our findings, these data suggest that loss of vSMC coverage is present in *Alk1*-deficient embryos, as well as in the *Alk1*-deficient adult mouse brain and human bAVM. How this commonality in phenotypes contributes to the pathogenesis or clinical sequelae remains to be elucidated.

During vessel assembly, sprouting endothelial tubes recruit mesenchymal progenitors that differentiate into vSMC or pericytes. The recruitment of pericytes to vessels indicates the maturation of a vascular system, as well as the establishment and maintenance of blood-brain barrier integrity.[9, 18] The importance of pericytes in maintaining cerebrovascular integrity in adults has been described by Bell et al.[19] Tu et al analyzed the ultrastructure of a specimen from an unruptured bAVM and found that pericytes were less common in perinidal capillaries than in control vessels.[14] The number of lysosomes and pinocytotic vesicles in the residual pericytes increased, indicating BBB opening. Caution is needed in interpreting these findings, as these changes may be epiphenomenal and are due to some process unrelated to the original pathogenesis of the lesion, e.g., some consequence of long-standing high flow rates in the vascular structures. Nonetheless, if these changes in human specimens are related to the pathogenesis, they are consistent with our findings. Here, we showed that the dysplastic vessels in the angiogenic foci of *Alk1*-deficient brain have a reduced number of pericytes associated with increased fibrinogen extravasation, suggesting that Alk1 is involved in mural cell recruitment during angiogenesis in the adult mouse brain. How Alk1 regulates this process needs to be clarified, and is a potentially important subject of future research.

PDGFR-β/PDGF-BB signaling regulates pericyte recruitment and differentiation to nascent capillaries. The differentiation of mesenchymal cells into the pericyte/vSMCs lineage is dependent on PDGFR-β expression in the mouse.[20] *Pdgfrβ* or *Pdgfb* null mice have cerebral hemorrhage with an absence of microvascular pericytes in the brain vessels and endothelial hyperplasia.[21] Here, we demonstrated that the expression of PDGFR-β was reduced in the angiogenic foci of *Alk1*-deficient mice, suggesting a possible link between Alk1 and PDGFR-β/PDGF-BB signal pathways. However, it is not clear whether the reduced expression of PDGFR-β is due to the reduced number of pericytes in the tissue. We found that PDGFR-β protein was reduced in the brain of untreated *Alk1*-deficient mice even though the number of vascular associated pericytes was not reduced, possibly because we used homogenous brain tissues. Gene expression by other cell-types may influence the analysis. Therefore, the specific effect of pericytes may not be accurately reflected in the protein analysis. The exact mechanism that links PDGFR-β/PDGF-BB signaling and Alk1 will require further investigation.

We did not detect any changes in PDGF-BB expression in the *Alk1*-deficient brain. Other than endothelial cells, PDGF-BB expression has been detected in the neurons of the adult rat brain.[22] Endothelial-specific *Pdgfb* deletion causes vSMC/pericyte deficiency, whereas its depletion in hematopoietic cells[23] or neurons[24] has no obvious effect on the vascular structure. Although our data suggest that *Alk1* deletion does not affect the level of PDGF-BB expression, it is possible that the neuronal expression of PDGF-BB in the adult brain masks the changes of endothelial cell-derived PDGF-BB. Lebrin et al showed that thalidomide upregulated PDGF-BB expression, increased mural cell coverage, and rescued vessel wall defects in Eng$^{+/-}$ mice.[25] These findings suggest that the alteration of PDGFR-β/PDGF-BB signaling could be one of the underlying mechanisms for HHT2-associated bAVM pathogenesis, and provide an impetus to develop new therapies.

This study has two limitations. (1) Because adenoviral vector itself could cause local inflammation, we could not determine in our current model whether vascular leakage leads to local inflammation or vice versa during the pathogenesis of the cerebrovascular dysplasia. We have now developed new models without local viral vector-injection. We would like to address those questions in the future using different models. (2) We don't know if loss of mural cell-coverage is a primary or secondary effect of *Alk1* deficiency. Additional experiments are needed to identify the primary cell type that causes this phenotype.

In conclusion, in a mouse model that simulates aspects of human bAVM, especially those associated with HHT2, we described and quantified a series of abnormalities consistent with compromised vascular integrity of the affected vasculature. A common theme was extravascular localization of intravascular components. The extravasation of intravascular components correlated with the reduction of vascular mural cells and increase of macrophage burden. Reduced expression of PDGFR-β in the angiogenic foci of *Alk1*-deficient brain suggests that PDGFR-β/PDGF-BB signaling could be involved in regulating mural cell recruitment in HHT2-associated bAVM. Modulation of PDGFR-β/PDGF-BB shows promise in the development of novel therapies to stabilize the abnormal vasculature and reduce the risk of HHT2-associated bAVM rupture.

Supplementary Material

Refer to Web version on PubMed Central for supplementary material.

Acknowledgments

References

1. Attia W, Tada T, Hongo K, Nagashima H, Takemae T, Tanaka Y, Kobayashi S. Microvascular pathological features of immediate perinidal parenchyma in cerebral arteriovenous malformations: giant bed capillaries. J Neurosurg. 2003; 98:823–827. [PubMed: 12691408]

2. Sato S, Kodama N, Sasaki T, Matsumoto M, Ishikawa T. Perinidal dilated capillary networks in cerebral arteriovenous malformations. Neurosurgery. 2004; 54:163–168. discussion 168-170. [PubMed: 14683554]

3. Kim H, Marchuk DA, Pawlikowska L, Chen Y, Su H, Yang GY, Young WL. Genetic considerations relevant to intracranial hemorrhage and brain arteriovenous malformations. Acta Neurochir Suppl. 2008; 105:199–206. [PubMed: 19066109]

4. Walker EJ, Su H, Shen F, Choi EJ, Oh SP, Chen G, Lawton MT, Kim H, Chen Y, Chen W, Young WL. Arteriovenous malformation in the adult mouse brain resembling the human disease. Ann Neurol. 2011; 69:954–962. [PubMed: 21437931]

5. Park SO, Wankhede M, Lee YJ, Choi EJ, Fliess N, Choe SW, Oh SH, Walter G, Raizada MK, Sorg BS, Oh SP. Real-time imaging of de novo arteriovenous malformation in a mouse model of hereditary hemorrhagic telangiectasia. J Clin Invest. 2009; 119:3487–3496. [PubMed: 19805914]

6. Shen F, Su H, Liu W, Kan YW, Young WL, Yang GY. Recombinant adeno-associated viral vector encoding human VEGF165 induces neomicrovessel formation in the adult mouse brain. Front Biosci. 2006; 11:3190–3198. [PubMed: 16720385]

7. Adams RA, Schachtrup C, Davalos D, Tsigelny I, Akassoglou K. Fibrinogen signal transduction as a mediator and therapeutic target in inflammation: lessons from multiple sclerosis. Curr Med Chem. 2007; 14:2925–2936. [PubMed: 18045138]

8. Armulik A, Genove G, Betsholtz C. Pericytes: developmental, physiological, and pathological perspectives, problems, and promises. Dev Cell. 2011; 21:193–215. [PubMed: 21839917]

9. Daneman R, Zhou L, Kebede AA, Barres BA. Pericytes are required for blood-brain barrier integrity during embryogenesis. Nature. 2010; 468:562–566. [PubMed: 20944625]

10. Sadick H, Naim R, Sadick M, Hormann K, Riedel F. Plasma level and tissue expression of angiogenic factors in patients with hereditary hemorrhagic telangiectasia. Int J Mol Med. 2005; 15:591–596. [PubMed: 15754019]

11. Arteriovenous Malformation Study Group. Arteriovenous malformations of the brain in adults. N Engl J Med. 1999; 340:1812–1818. [PubMed: 10362826]

12. Prayer L, Wimberger D, Stiglbauer R, Kramer J, Richling B, Bavinzski G, Czech T, Imhof H. Haemorrhage in intracerebral arteriovenous malformations: detection with MRI and comparison with clinical history. Neuroradiology. 1993; 35:424–427. [PubMed: 8377912]

13. Guo Y, Saunders T, Su H, Kim H, Akkoc D, Saloner DA, Hetts SW, Hess C, Lawton MT, Bollen AW, Pourmohamad T, McCulloch CE, Tihan T, Young WL. Silent intralesional microhemorrhage as a risk factor for brain arteriovenous malformation rupture. Stroke. 2012; 43:1240–1246. [PubMed: 22308253]

14. Tu J, Stoodley MA, Morgan MK, Storer KP. Ultrastructure of perinidal capillaries in cerebral arteriovenous malformations. Neurosurgery. 2006; 58:961–970. discussion 961-970. [PubMed: 16639333]

15. Chen Y, Zhu W, Bollen AW, Lawton MT, Barbaro NM, Dowd CF, Hashimoto T, Yang GY, Young WL. Evidence of inflammatory cell involvement in brain arteriovenous malformations. Neurosurgery. 2008; 62:1340–1349. [PubMed: 18825001]

16. Kim H, Hysi PG, Pawlikowska L, Poon A, Burchard EG, Zaroff JG, Sidney S, Ko NU, Achrol AS, Lawton MT, McCulloch CE, Kwok PY, Young WL. Common variants in interleukin-1-beta gene are associated with intracranial hemorrhage and susceptibility to brain arteriovenous malformation. Cerebrovasc Dis. 2009; 27:176–182. [PubMed: 19092239]

17. Oh SP, Seki T, Goss KA, Imamura T, Yi Y, Donahoe PK, Li L, Miyazono K, ten Dijke P, Kim S, Li E. Activin receptor-like kinase 1 modulates transforming growth factor- beta 1 signaling in the regulation of angiogenesis. Proc Natl Acad Sci U S A. 2000; 97:2626–2631. [PubMed: 10716993]

18. Armulik A, Genove G, Mae M, Nisancioglu MH, Wallgard E, Niaudet C, He L, Norlin J, Lindblom P, Strittmatter K, Johansson BR, Betsholtz C. Pericytes regulate the blood-brain barrier. Nature. 2010; 468:557–561. [PubMed: 20944627]

19. Bell RD, Winkler EA, Sagare AP, Singh I, LaRue B, Deane R, Zlokovic BV. Pericytes control key neurovascular functions and neuronal phenotype in the adult brain and during brain aging. Neuron. 2010; 68:409–427. [PubMed: 21040844]

20. Crosby JR, Seifert RA, Soriano P, Bowen-Pope DF. Chimaeric analysis reveals role of Pdgf receptors in all muscle lineages. Nat Genet. 1998; 18:385–388. [PubMed: 9537425]

21. Hellstrom M, Gerhardt H, Kalen M, Li X, Eriksson U, Wolburg H, Betsholtz C. Lack of pericytes leads to endothelial hyperplasia and abnormal vascular morphogenesis. J Cell Biol. 2001; 153:543–553. [PubMed: 11331305]

22. Sasahara M, Sato H, Iihara K, Wang J, Chue CH, Takayama S, Hayase Y, Hazama F. Expression of platelet-derived growth factor B-chain in the mature rat brain and pituitary gland. Brain Res Mol Brain Res. 1995; 32:63–74. [PubMed: 7494464]

23. Kaminski WE, Lindahl P, Lin NL, Broudy VC, Crosby JR, Hellstrom M, Swolin B, Bowen-Pope DF, Martin PJ, Ross R, Betsholtz C, Raines EW. Basis of hematopoietic defects in platelet-derived growth factor (PDGF)-B and PDGF beta-receptor null mice. Blood. 2001; 97:1990–1998. [PubMed: 11264163]

24. Enge M, Wilhelmsson U, Abramsson A, Stakeberg J, Kuhn R, Betsholtz C, Pekny M. Neuron-specific ablation of PDGF-B is compatible with normal central nervous system development and astroglial response to injury. Neurochem Res. 2003; 28:271–279. [PubMed: 12608700]

25. Lebrin F, Srun S, Raymond K, Martin S, van den Brink S, Freitas C, Breant C, Mathivet T, Larrivee B, Thomas JL, Arthur HM, Westermann CJ, Disch F, Mager JJ, Snijder RJ, Eichmann A, Mummery CL. Thalidomide stimulates vessel maturation and reduces epistaxis in individuals with hereditary hemorrhagic telangiectasia. Nat Med. 2010; 16:420–428. [PubMed: 20364125]
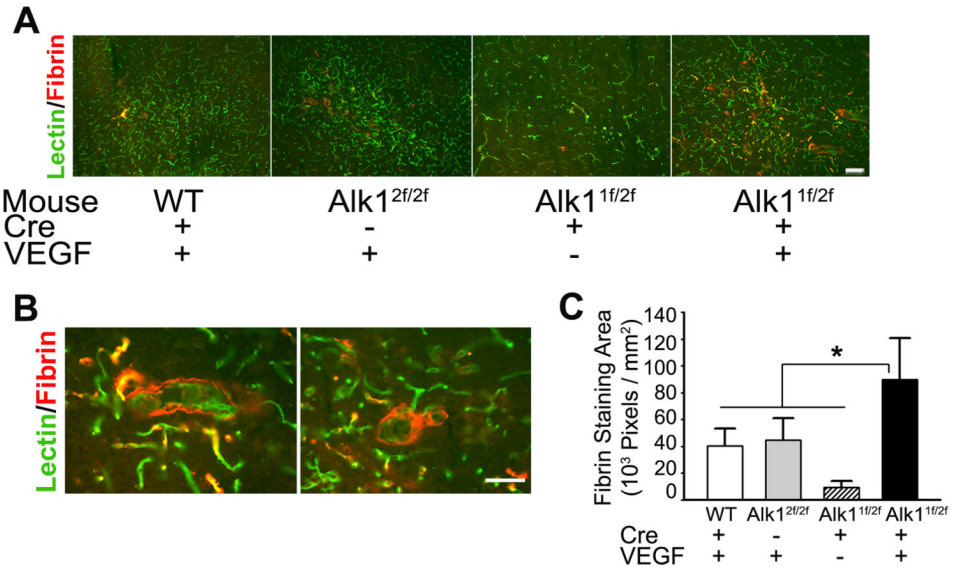
Figure 1.
The dysplastic vessels in the angiogenic foci of *Alk1*-deficient brain have increased permeability than vessels in the angiogenic foci of the normal brain. (A) Representative images show vessels (lectin, green) and fibrin (red) in the viral-injected region. (B) High magnification images show the location of fibrin. The fibrin lines outside the dysplastic vessel wall in the *Alk1*-deficient brain. (C) Bar graph shows the quantification of fibrin. In the viral-injected region, there were significantly more fibrin deposition in the VEGF-treated *Alk1*-deficient brain than VEGF-treated WT (*p= 0.001) and *Alk1*$^{2f/2f}$ (*p= 0.003) groups, and *Alk1*-deficient brain without VEGF treatment (*p<0.001). Scale bars: 50 μm.
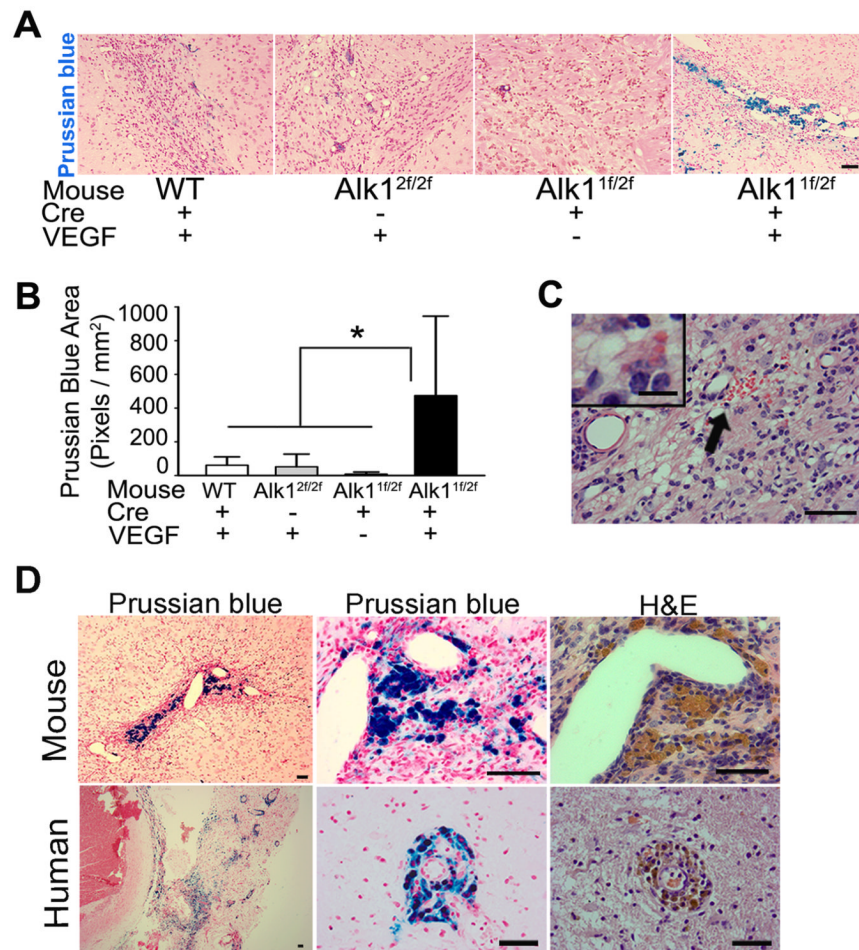
Figure 2.
RBCs and iron deposition were detected around the dysplastic vessels. (A) Representative images of Prussian blue staining show the iron deposition around dysplastic vessels in the angiogenic foci of *Alk1*-deficient brain. (B) Bar graph shows the quantification of Prussian blue-positive area. The VEGF-stimulated *Alk1*-deficient group had significantly increased Prussian blue-positive area than VEGF-treated WT (*p=0.04) and *Alk1*$^{2f/2f}$ (*p=0.03) group, and untreated *Alk1*-deficient brain (*p=0.02). (C) RBCs were found in extravascular space (black arrow). Scale bar: 50 µm. The insert shows a macrophage with three red blood cells in its cytoplasm. Scale bar in the insert: 10 µm. The brain was perfused with PBS before collection. (D) Representative images of hematoxylin and eosin (H&E) and Prussian blue stained *Alk1*-deficient mouse and human bAVM sections. Hemosiderin and Prussian blue-positive staining were detected around dysplastic vessels in the angiogenic foci of *Alk1*-deficient brain and in the human bAVM. Scale bars: 50 µm.
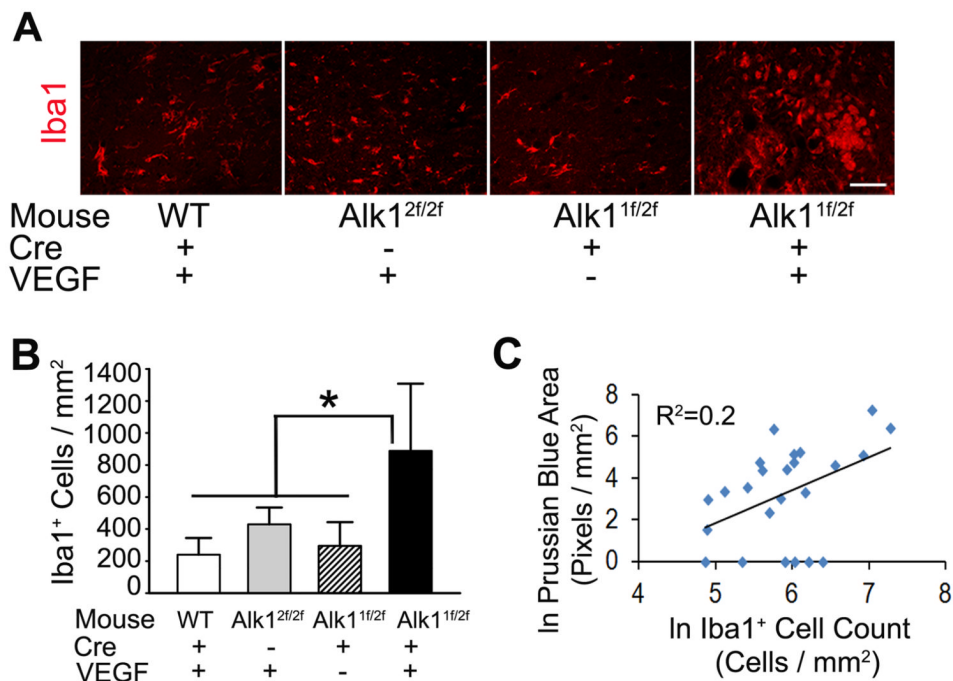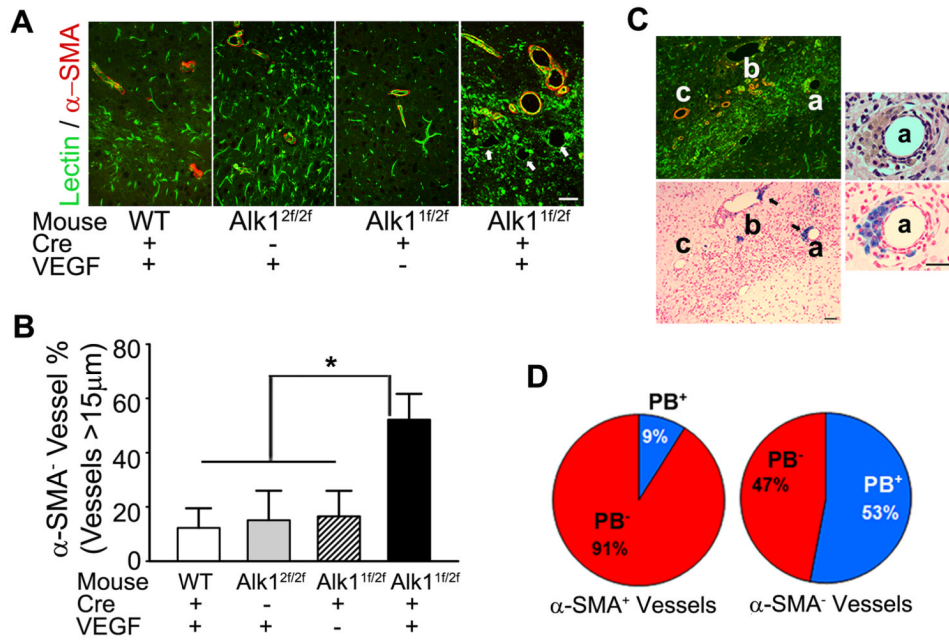
Figure 3.
Prussian blue staining positively correlated with macrophage/microglia infiltration. (A) Representative images of Iba1 antibody staining (red). Scale bar: 50 μm. (B) Bar graph shows quantification of Iba1$^+$ cells. The VEGF-stimulated *Alk1*-deficient group had more Iba1$^+$ cells than VEGF-treated WT (*p=0.001) and *Alk1*$^{2f/2f}$ (*p=0.015) groups, and untreated *Alk1*-deficient-group (*p=0.002). (C) Graph shows Prussian blue-positive area positively correlated with the number of Iba1$^+$ cells (R^2=0.2, *p<0.05).

Figure 4.
The dysplastic vessels in the angiogenic foci of *Alk1*-deficient brain had less coverage of α-SMA⁺ cells. (A) Representative images of lectin (green) and anti-αSMA (red) stained sections. In the angiogenic foci of *Alk1*-deficient brain, some vessels larger than 15 μm had no α-SMA⁺ cells (white arrows). Scale bar: 50 μm. (B) Bar graph shows the percentage of α-SMA⁻ vessels (>15 μm). Significantly more α-SMA⁻ vessels presented in the VEGF-stimulated *Alk1*-deficient brain than that in WT (*p<0.001), *Alk1*²ᶠ/²ᶠ (*p<0.001) and *Alk1*-deficient-only (*p<0.001) groups. (C) Prussian Blue stains were detected around α-SMA⁻ vessels. The left panel shows Prussian blue-positive staining around the α-SMA⁻ vessels, such as Vessels a and b (black arrows). Scale bars: 50 μm. The right panel shows high magnification images of Vessel a from the left panel. H&E (top) and Prussian blue (bottom) stained sections. Brown colored cells around vessels are hemosiderin positive macrophages. Scale bars: 30 μm. (D) Pie graphs show significantly more PB⁺ vessels are α-SMA⁻ vessels (*p<0.001). PB: Prussian blue.
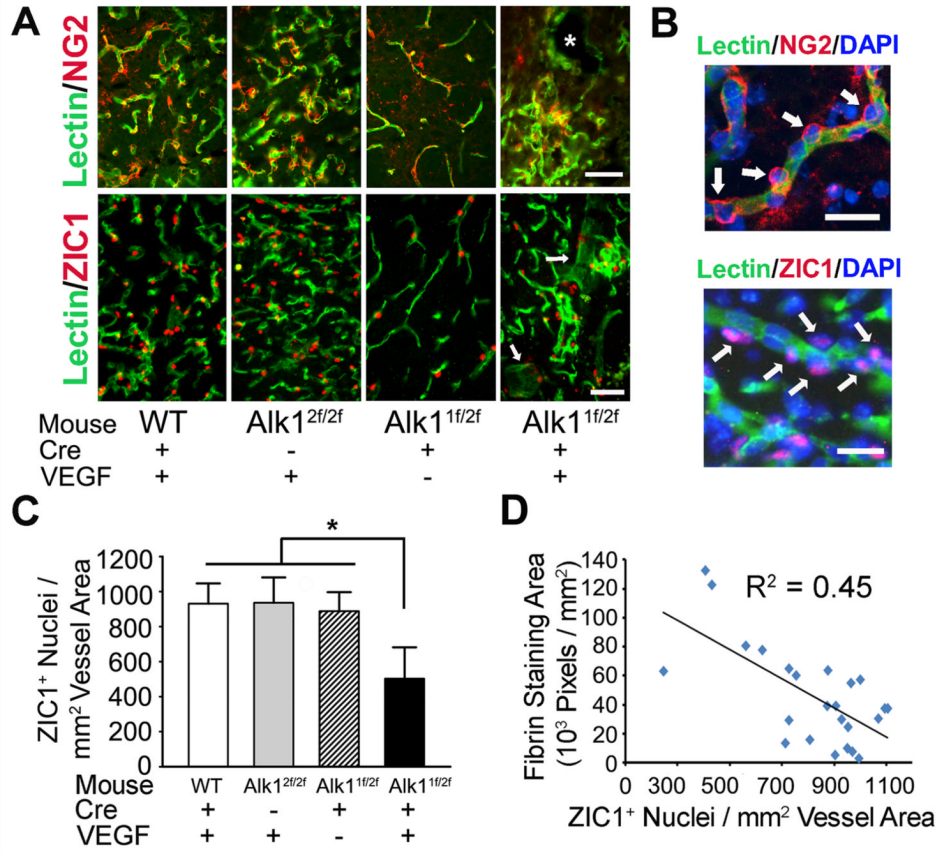
Figure 5.
The dysplastic vessels in the angiogenic foci of *Alk1*-deficient brain have fewer pericytes on their walls. (A) Representative images show vessels (lectin, green) and pericytes (upper panel: NG2, red; lower panel: vascular associated ZIC1$^+$ cells, red) in the vector injection sites. * in upper panel and arrows in lower panel indicate dysplastic vessels. Scale bars: 50 μm. (B) High magnification images of pericytes. The upper panel shows vascular (green) associated NG2+ pericyte (arrows, red). The lower panel shows the ZIC1$^+$ pericytes (arrows, red) co-localized with nuclei (DAPI, blue). Scale bars: 20 μm. (C) Bar graph shows the quantification of pericytes located on the vessel wall. (D) Graph shows the number of vessel-associated pericyte inversely correlating with the degree of fibrin deposition (R^2 =0.45).